Overburden geomechanical effects on 4D seismic response – influences of stiffness contrast, anisotropy and geometry

Liming Li[1], Andreas Bauer[2], Rune M Holt[3], Erling Fjær[2], Jørn F Stenebråten[1], Audun Bakk[1]*

[1] *SINTEF Petroleum Research*

[2] *SINTEF Petroleum Research and Norwegian University of Science and Technology*

[3] *Norwegian University of Science and Technology and SINTEF Petroleum Research*

Summary

Petroleum production and CO_2 storage induce effective stress changes and deformations in the reservoir, as well as in the overburden. This may be detected by 4D seismic monitoring due to the stress-sensitivity of the seismic velocities in the rocks. Here we address how stiffness contrast between the reservoir rock and the overburden, reservoir inclination, and overburden rock anisotropy may affect changes in two-way seismic travel time, based on laboratory measured stress-sensitivity of wave velocities in rock specimens and field scale geomechanical modeling.

Introduction

Pore pressure changes caused by reservoir depletion or inflation by fluid injection lead to stress changes within the reservoir and in the surrounding rocks. Resulting effective stress changes will alter the seismic properties of the rocks involved (Hornby, 1998; Sayers, 2002; Prioul *et al.*, 2004; Ciz & Shapiro, 2009). This makes time lapse seismic an important tool to monitor subsurface alterations (*e.g.*, Landrø 2001) and thereby improving recovery or storage capacity by optimal placement of new wells. Since seismic waves propagate twice through usually very thick overburden, overburden changes become significant and have to be understood in order to properly interpret 4D seismic data (Kenter *et al.*, 2004; Hatchell & Bourne, 2005; Fjær & Kristiansen, 2009; Herwanger & Home, 2009).

Subsurface stress alterations induced by pore pressure changes are primarily related to the geometry (shape and orientation) of the depleted / inflated volume, and to rock mechanical properties of the reservoir and its surroundings. In this work we address how elastic contrast in stiffness between the reservoir rock and the overburden, rock anisotropy, and the inclination of the reservoir influence the stress changes, and furthermore how the seismic two-way travel time (TWT) is influenced. Additional influence associated with rock heterogeneity and non-elastic effects (plastic deformation, faulting / fault reactivation) is not considered in this paper.

Geomechanical modeling

Stress changes around a depleting reservoir can be estimated analytically by use of Geertsma's nucleus of strain model (1973) for a linearly elastic and isotropic homogeneous subsurface (no elastic contrast between the reservoir and its surroundings). This method can be extended to complex reservoir geometry by integrating on a numerically discretized reservoir.

However, numerical modeling is needed in more general conditions, for example, when fluid coupling, rock non-linear elasticity, plasticity, anisotropy, heterogeneity and discontinuity have to be taken into consideration. In this work, the analyses of the subsurface stress and stress changes have been carried out using the finite element method (FEM) (*e.g.*, Zienkiewicz and Taylor, 2005). In a FEM model, the geological units are discretized into elements. The elements are connected through nodes. The deformation of each element is related to the node forces, according to the material constitutive behavior which may be derived from laboratory measurements on rock specimens. Reasonable estimates can thus be made using a model which properly mimics the geometry, the initial conditions, the boundary conditions and the mechanical properties of the rocks.

Experimental rock physics

With the results of the stress analysis, we also need a rock physics model or a relation which links the changes of the stress and the changes of the seismic wave velocities, in order to quantify the geomechanical effects on 4D seismic. It is essential, since the velocities depend strongly on stress path (*e.g.* Holt *et al.*, 2005), to obtain stress sensitivity from laboratory measurements along an appropriate stress path for *in situ* conditions.

An example is shown in Figure 1, where an undrained constant mean stress path was applied to a sample of Pierre Shale, mimicking the case of no elastic contrast between the reservoir and the cap rock. The axial stress (σ_z) was decreased step-wise and the sample permitted to equilibrate. The resulting sensitivity of the axial P-wave velocity (v_{Pz}) with decreasing axial stress was found to be

$$S = \frac{\Delta v_{Pz}}{v_P \Delta \sigma_z} \approx 3\, GPa^{-1} \qquad (1)$$

S (Bauer *et al.*, 2008) will vary with shale characteristics like porosity and clay content, in addition to stress level

DOI http://dx.doi.org/10.1190/segam2014-1530.1

and stress path. There is currently no calibrated rock physics model nor sufficiently complete data base for stress dependent velocities in shale along representative *in situ* stress paths. In the following we will hence lean on the value obtained with Pierre shale, which is of the same order of magnitude as measured in other overburden shales. The predicted stress-induced changes in two-way seismic travel time appear to scale linearly with the value of *S*, so one may easily estimate the effect of having a more or less stress sensitive shale.

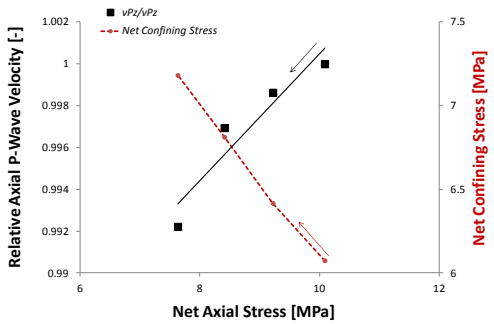

Figure 1. Ultrasonic axial P-wave velocity measured vs. net axial stress during a constant mean stress test with Pierre Shale (sample axis normal to the bedding plane). The total axial stress, confining pressure and pore pressure were initially 20, 16 and 10 MPa, respectively (i.e. net initial axial stress = 10 MPa). Also shown is the corresponding change in net confining pressure. Velocity data were acquired throughout the whole test, but only the measurements taken at the end of each consolidation interval can be used to assess the stress dependence.

Effects of elastic contrast and of reservoir inclination

Mulders (2003) used FEM modeling to assess the overburden stress path while the reservoir was depleted. The stress path is described by the coefficients γ_v and γ_h (Hettema *et al.*, 2000), defined as

$$\gamma_v = \frac{\Delta\sigma_v}{\Delta p_{f,res}};\quad \gamma_h = \frac{\Delta\sigma_h}{\Delta p_{f,res}} \qquad (2)$$

Here $\Delta\sigma_v$ and $\Delta\sigma_h$ are vertical and horizontal stress changes, respectively, and $\Delta p_{f,res}$ is the pore pressure change in the reservoir. γ_v is referred to as an "arching" (Kenter *et al.*, 2004) coefficient, since it describes the shielding of the reservoir by stress arching in the overburden.

Building on correlations (Mahi, 2003) with the FEM simulations referred above, the effects of elastic contrast and reservoir tilt on the stress path coefficients may be addressed in a systematic way. Figure 2 shows the effect of elastic contrast. In the base case (Geertsma's model), the mean stress is almost zero, so that $\gamma_v + 2\gamma_h = 0$. Positive γ_v means that the vertical stress is reduced for pore pressure depletion ($\Delta p_{f,res} < 0$) (notice that the resulting γ_h is approximated in a less rigorous manner than γ_v and appears as linear trendlines – for the purpose of this work, this is sufficient).

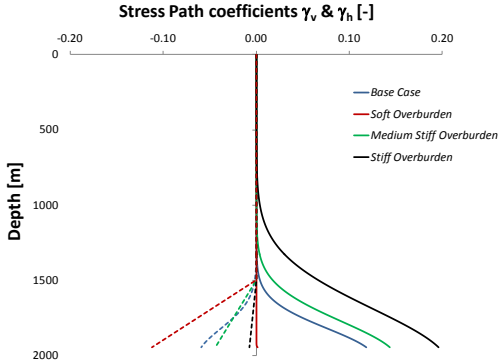

Figure 2. Stress path coefficients γ_v (solid line) and γ_h (dashed line) vs. depth for 4 cases with varying elastic contrast between cap and reservoir rock (see Table 1). Top of reservoir is at 1950m depth, and the reservoir is disk-shaped with a depleted zone of 100m thickness and 500m diameter.

Notice that increasing stiffness of the overburden leads to more stress arcing, i.e. larger vertical stress decrease in the overburden. The zone of influence also extends upwards. With softer overburden, the effect is opposite. On the other hand, in the latter case the mean stress is increased, which may lead to undrained pore pressure increase in the overburden. Beyond representing a risk for potential drilling hazards, this may also have a direct impact on 4D seismic response, as seen below.

We may now estimate the change in two-way seismic travel time for a fictitious case of a homogeneous overburden above a depleting reservoir, undergoing stress changes as predicted by Figure 2. The vertical P-wave velocity will then primarily be reduced as a result of the vertical stress reduction. In case of mean stress change, the pore pressure may change in the overburden: If it increases, this contributes to a further reduction of the velocity, whereas if it decreases, it reduces the velocity drop. Figure 3 shows the calculated ΔTWT vs. depth for the same scenarios as in Figure 2, also including a hypothetical case where the full change in mean stress is transferred into a pore pressure change. Figure 3 shows that largest 4D effects are seen for a stiff overburden, in which case the mean stress is reduced, and a pore pressure effect would reduce ΔTWT. In case of a soft overburden, pore pressure increase magnifies the 4D effect.

A significant effect is observed if the reservoir is tilted (Figure 4). An inclination of 10° nearly doubles the ΔTWT, even in the absence of elastic contrast.

DOI http://dx.doi.org/10.1190/segam2014-1530.1

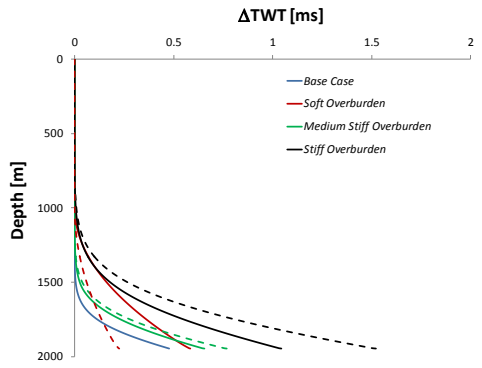

Figure 3: Change in *ΔTWT* vs. depth for the same cases as shown in Figure 2, and with a stress sensitivity S = 3 GPa^{-1} in the overburden. Solid curves: Effect of pore pressure change = mean stress change included; dashed curves: No pore pressure effect.

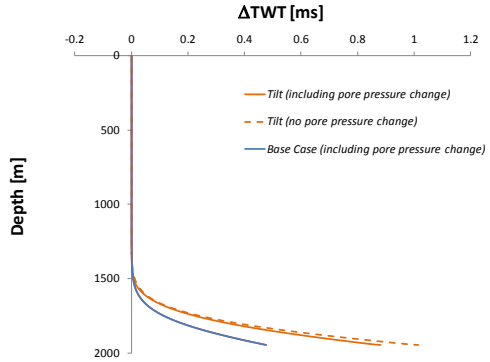

Figure 4: Change in *ΔTWT* vs. depth for the base case and for a tilted reservoir (10°) (also matched to the surrounding). Cap rock stress sensitivity S = 3 GPa^{-1}.

Table 1: Stress path coefficients γ_v and γ_h and changes in TWT at top of the reservoir (1950 m depth) for different cases used in the simulations. Reservoir E-modulus is 7.6 GPa in all cases, whereas the E-modulus of the cap rock is varied as shown in the Table. Poisson's ratio = 0.23 for both reservoir and overburden, except for the Soft overburden, which has properties similar to Pierre Shale, and therefore Poisson's ratio = 0.39. Notice that *ΔTWT* is calculated for hypothetical cases of no pore pressure change (Δp_f=0) and pore pressure change equal to the change in mean stress ($\Delta p_f \neq 0$).

	E_{cap} [GPa]	γ_v	γ_h	$\Delta TWT_{\Delta p_f=0}$ [ms]	$\Delta TWT_{\Delta p_f\neq 0}$ [ms]
Base	7.6	0.12	-0.06	0.48	0.48
Medium	10	0.14	-0.04	0.77	0.66
Stiff	15	0.20	-0.01	1.52	1.04
Soft	0.77	0.00	-0.11	0.21	0.55
Tilt 10°	7.6	0.25	-0.06	1.02	0.88

Effects of elastic anisotropy in the overburden

Geomechanical modeling was performed to address the impact of overburden shale anisotropy on stress path and on resulting TWT in a 4D survey, using commercially available software (ABAQUS). The model setup includes a reservoir with a rectangular plate shape, with horizontal dimensions 500 x 500 m^2 and a thickness of 100 m. The top of the reservoir is 2000 m below the surface. With the reservoir in the center, the models simulate a block of rock with dimensions 3500 x 3500 m^2 in the horizontal plane and a total depth of 4100 m.

We simulated two cases. In case I (called isotropic case), the rocks in the whole model are isotropic. This represents using *E*-modulus and Poisson's ratio measured from a core which is taken normal to the bedding plane, without the awareness of anisotropy. In case II (called anisotropic case), the overburden and sideburden are transversely isotropic, while the rest part of the model is isotropic.

As input parameters for a transversely isotropic stiff cap rock we used the data published by Søreide *et al*. (2009). Those data were from measurements on shale cores from offshore Norway. We used a data set obtained from measurements at 20 MPa confining stress. The values are listed in Table 2, along with corresponding data representative of a soft overburden. Here we used data obtained for Pierre Shale in our laboratory.

In both cases, the reservoir and the surrounding rocks were given the same properties; the reservoir was however always isotropic.

Table 2: Input elastic parameters for stiff and soft shales, including anisotropic E-moduli and Poisson's ratios. Subscript t denotes transversal (i.e. normal to the bedding plane), while subscript p denotes parallel to bedding. The table also shows the computed stress path coefficients, and the changes in TWT at top of the reservoir (2000m depth). Notice that *ΔTWT* is calculated for hypothetical cases of no pore pressure change (Δp_f=0) and pore pressure change equal to the change in mean stress ($\Delta p_f \neq 0$).

	E_t, ν_{tp} [GPa]	E_p, ν_p [GPa]	γ_v	γ_h	$\Delta TWT_{\Delta p_f=0}$ [ms]	$\Delta TWT_{\Delta p_f\neq 0}$ [ms]
Isotropic (stiff)	7.6, 0.23	7.6, 0.23	0.12	-0.06	0.58	0.58
Anisotropic (stiff)	7.6, 0.23	14.1, 0.14	0.11	-0.09	0.57	0.59
Isotropic (soft)	0.77, 0.39	0.77, 0.39	0.06	-0.03	0.45	0.45
Anisotropic (soft)	0.77, 0.39	1.5, 0.36	0.05	-0.04	0.52	0.46

Figure 5. shows the stress path coefficients γ_v and γ_h, plotted against the depth. There is very little difference for

DOI http://dx.doi.org/10.1190/segam2014-1530.1

γ_v between the isotropic case and the anisotropic case. It indicates that the anisotropy has little effect on the vertical stress. Consequently, the difference of ΔTWT between two cases is negligible, as shown in Figure 6. However, the anisotropy has a significant impact on the horizontal stress changes (ref. Figure 5). The effects on wave propagation may thus be expected in case of non-zero offset. This may not directly affect calculated two way time, but will affect seismic data processing in general and affect AVO analysis.

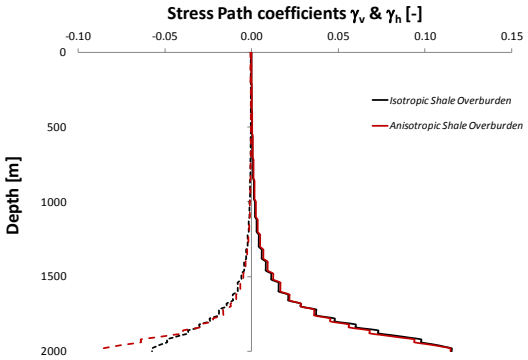

Figure 5. Stress path coefficients γ_v (solid line) and γ_h (dashed line) vs. depth for a stiff overburden above a depleting reservoir, including cases of isotropic and anisotropic rock properties (see Table 2). Top of reservoir is at 2000m depth, and the reservoir has rectangular plate shape with a depleted zone of 100m thickness and 500m x 500m in lateral extent.

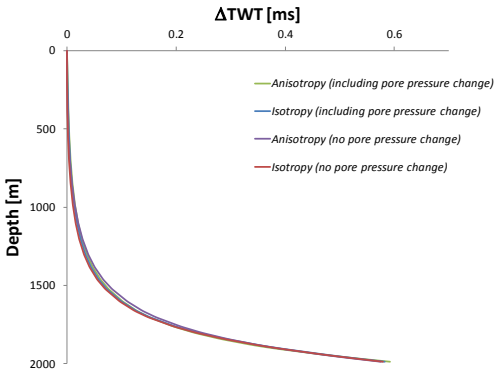

Figure 6: Change in ΔTWT vs. depth for 10 MPa depletion, plotted for the same cases as shown in Figure 5, and with a stress sensitivity S = 3 GPa^{-1} in the overburden.

Conclusions

We have investigated to what extend stress changes above a depleting reservoir and two-way seismic travel times are affected by stiffness contrast between reservoir and overburden, reservoir tilt, and rock anisotropy. The effect of anisotropy in the overburden turns out to be relatively small for vertically propagating seismic waves. Stiffness contrast between reservoir and overburden, as well as a tilt of the reservoir, however, result in significant changes in vertical, horizontal, and mean stress. Vertical p-wave velocity and TWT are mostly affected by vertical effective stress changes, which means that besides vertical total stress changes also pore-pressure changes caused by mean stress changes (in a low permeability formation) will have a strong impact on TWT.

Acknowledgements

The authors wish to acknowledge The Norwegian Research Council and funding industrial partners for support through the JIP " Shale rock physics: Improved seismic monitoring for increased recovery" at SINTEF and through the ROSE Program at NTNU.

DOI http://dx.doi.org/10.1190/segam2014-1530.1

http://dx.doi.org/10.1190/segam2014-1530.1

EDITED REFERENCES

Note: This reference list is a copy-edited version of the reference list submitted by the author. Reference lists for the 2014 SEG Technical Program Expanded Abstracts have been copy edited so that references provided with the online metadata for each paper will achieve a high degree of linking to cited sources that appear on the Web.

REFERENCES

Bauer, A., C. Lehr, F. Korndorffer, A. van der Linden, J. Dudley, T. Addis, K. Love, and M. Myers, 2008, Stress and pore pressure dependence of sound velocities in shales: Poroelastic effects in time-lapse seismic: Presented at the 78th Annual International Meeting, SEG.

Ciz, R., and S. A. Shapiro, 2009, Stress-dependent anisotropy in transversely isotropic rocks: Comparison between theory and laboratory experiment on shale : Geophysics, **74**, no. 1, D7–D12, http://dx.doi.org/10.1190/1.3008546.

Fjær, E., and T. G. Kristiansen, 2009, An integrated geomechanics, rock physics, and seismic model: Presented at the 71st Annual International Conference and Exhibition, EAGE.

Geertsma, J., 1973, A basic theory of subsidence due to reservoir compaction: The homogeneous case: Transactions of Royal Dutch Society of Geology & Mining Engineering, **22**, 43–62.

Hatchell, P., and S. Bourne, 2005, Rocks under strain: Strain-induced time-lapse time shifts are observed for depleting reservoirs: The Leading Edge, **24**, 1222–1225, http://dx.doi.org/10.1190/1.2149624.

Herwanger, J. V., and S. A. Horne, 2009, Linking reservoir geomechanics and time-lapse seismics: Predicting anisotropic velocity changes and seismic attributes: Geophysics, **74**, no. 4, W13–W33, http://dx.doi.org/10.1190/1.3122407.

Holt, R. M., O.-M. Nes, and E. Fjær, 2005, In-situ stress dependence of wave velocities in reservoir and overburden rocks: The Leading Edge, **24**, 1268–1274, http://dx.doi.org/10.1190/1.2149650.

Hornby, B. E., 1998, Experimental laboratory determination of the dynamic elastic properties of wet drained shales: Journal of Geophysical Research, **103**, B12, 29945–29964, http://dx.doi.org/10.1029/97JB02380.

Kenter C.J., A.C. Van den Beukel, P.J. Hatchell, K.P. Maron, M.M. Molenaar, and J.G.F Stammeijer, 2004, Geomechanics and 4D: Evaluation of reservoir characteristics from time shifts in the overburden: ARMA/NARMS 04-627, Proceedings of Gulf Rocks 2004.

Landrø, M., 2001, Discrimination between pressure and fluid saturation changes from time-lapse seismic data: Geophysics, **66**, 836–844, http://dx.doi.org/10.1190/1.1444973.

Mahi, A., 2003, Stress path of depleting reservoirs: M.Sc. thesis, Norwegian University of Science and Technology.

Mulders, F. M. M., 2003, Modeling of stress development and fault slip in and around a producing gas reservoir: Ph.D. thesis, Delft University of Technology.

Prioul, R., A. Bakulin, and V. Bakulin, 2004, Nonlinear rock physics model for estimation of 3D subsurface stress in anisotropic formations: Theory and laboratory verification: Geophysics, **69**, 415–425, http://dx.doi.org/10.1190/1.1707061.

Sayers, C. M., 2002, Stress-dependent elastic anisotropy of sandstones: Geophysical Prospecting, **50**, no. 1, 85–95, http://dx.doi.org/10.1046/j.1365-2478.2002.00289.x.

Søreide, O. K., B. Bostrøm, and P. Horsrud, 2009, Borehole stability simulations of an HPHT field using anisotropic shale: 43rd U. S. Rock Mechanics Symposium and Fourth U. S.-Canada Rock Mechanics Symposium, ARMA 09-185.

Zienkiewicz, O. C., and R. L. Taylor, 2005, The finite element method for solid and structural mechanics, 6th ed.: Elsevier.